ELSEVIER

Journal of Crystal Growth 169 (1996) 747–751

JOURNAL OF CRYSTAL GROWTH

Growth and characterization of $Cd_{1-x-y}Zn_xMn_yTe$ crystals

W.C. Chou [a,*], F.R. Chen [a], T.Y. Chiang [a], H.Y. Shin [b], C.Y. Sun [b], C.M. Lin [c], K. Chern-Yu [c], C.T. Tsai [c], D.S. Chuu [c]

[a] *Department of Physics, Chung Yuan Christian University, Chung-Li 32023, Taiwan, ROC*
[b] *Department of Electronic Engineering, National Taiwan Institute of Technology, Taipei, Taiwan, ROC*
[c] *Department of Electro-Physics, National Chiao Tung University, Hsinchu 30049, Taiwan, ROC*

Received 20 November 1995; accepted 30 May 1996

Abstract

The $Cd_{1-x-y}Zn_xMn_yTe$ crystals, having potential in the development of magnetic field sensitive devices, were grown by the temperature gradient solution method at 940°C. All crystals were p-type with resistivity of $10^7\ \Omega \cdot cm$. They have novel magneto-optical properties, and could be substitutes for the $Cd_{1-x}Zn_xTe$ ternary compounds in certain optoelectronic/integrated-optical device applications.

1. Introduction

Over the past two decades, detailed studies have been performed on the Mn-based II–VI diluted magnetic semiconductors (DMS) [1,2] ternary compounds, $A_{1-x}Mn_xB$. The major concern of the studies can be divided into two categories. One is the sp–d exchange interaction, which characterizes the interesting optical and transport properties, such as giant Faraday rotation [3], magnetic field induced band splitting [4], polaron effect [5] and the magnetic field induced metal insulator transition [6]. The other is the d–d exchange interaction, which is the driving mechanism for the spin-glass phenomena [7] and Curie–Weiss behaviour [8].

Recently, the DMS quaternary compounds have attracted more attention than the ternary compounds [9,10]. The quaternary compounds have more controllable parameters than the ternary compounds. For example, both the lattice constant and the bandgap of the quaternary compounds can be managed in an arbitrary fashion. Whereas, for the ternary compound, the bandgap either increases or decreases with the shortening of lattice constant. Hence, the quaternary compounds, $Cd_{1-x-y}Zn_xMn_yTe$, are better candidates than the ternary compound $Cd_{1-x}Mn_xTe$ for the fabrication of optoelectrical devices and magnetic field sensor [11] or for the usage as the substrate for the unstrained devices.

Moreover, the quaternary compound bridges the two types of ternary compounds. For example, $Cd_{1-x-y}Zn_xMn_yTe$ interfaces $Cd_{1-x}Mn_xTe$ and $Zn_{1-y}Mn_yTe$. It is interesting to study the variation of the sp–d as well as the d–d exchange interaction as the host non-magnetic semiconductor changes from CdTe to CdZnTe then ZnTe. However, little effort has been devoted to the growth of $Cd_{1-x-y}Zn_xMn_yTe$ crystals.

In this study, the $Cd_{1-x-y}Zn_xMn_yTe$ crystals were grown by the temperature gradient solution

* Corresponding author.

PII S0022-0248(96)00452-6

method. The molar fraction of the constituent atoms were determined by an electron probe microanalyzer (EPMA). The resistivity, X-ray, and etch pit density (EPD) measurement were also performed to characterize the samples for further device application. The optical properties of the $Cd_{1-x-y}Zn_xMn_yTe$ crystals were studied by the reflectivity (R) and photoluminescence (PL) experiments. Finally, we have carried out the magnetization measurements to study the magnetic properties for the potential application in the magnetic field sensitive detector.

2. Experiment

The quaternary crystals $Cd_{1-x-y}Zn_xMn_yTe$ were grown by the temperature gradient solution method with the temperature gradient close to 50°C/cm. The temperature profile is shown in Fig. 1. In this work, the tellurium element was used as the solvent, the anion (Te^{2-}) to cation (Cd^{2+}, Zn^{2+}, and Mn^{2+}) molar ratio was 7 to 3, to lower the growth temperature from the congruent melting temperature of CdTe (1097°C) or ZnTe (1303°C) [12] to the temperature around 940°C. The large temperature gradient enables the impurities and excess Te to segregate to the higher temperature region. The other advantage is that the lower growth temperature prohibits the production of impurity from the growth ampoule at high temperature and avoids the evaporation of a large amount of Cd.

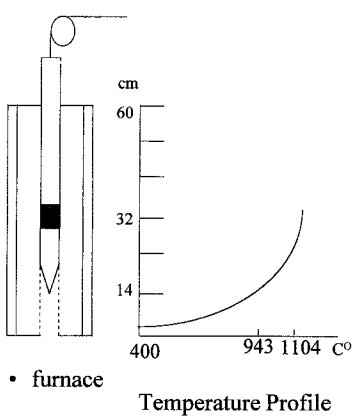

Fig. 1. The furnace set-up and temperature profile for the crystal growth.

The commercially available Te(6N) was purified by the zone refining method. The high purity Te was then loaded with a proper amount of Cd(6N), Zn(6N), and Mn(4N) elements in the graphite-coated quartz ampoule with a diameter of 15 mm. The ampoule was then evacuated to 10^{-6} Torr and sealed by a flame. For the chlorine-doped growth, a proper amount (100 to 5000 ppm) of $CdCl_2$ was also sealed within the ampoule. The pre-growth heating took 24 h with the lowest part of the ampoule located at 940°C, 14 cm away from the lowest exit of the furnace. After one day of the pre-heating process, the motor was started with a lowering rate of 2 cm/day. The post-growth cooling was carried out just after the completion of the solidification. The obtained crystals were about 10 cm in length with 30% of the $Cd_{1-x-y}Zn_xMn_yTe$ crystals and the rest was the Te element containing a large amount of impurity. For further studies, the crystals were sliced into 2 mm thick pieces then polished by the Al_2O_3 powder and 5% bromine–methanol solution.

3. Results and discussion

The molar fraction of constituent atoms for the $Cd_{1-x-y}Zn_xMn_yTe$ crystals were determined by the electron probe microanalyzer and were checked by lattice constant analysis using the X-ray diffraction and the optical measurements of the bandgap. The variation of the Zn concentration in the $Cd_{1-x}Zn_xTe$ ($Cd_{1-x-y}Zn_xMn_yTe$, $y = 0$) ternary compound along the growth direction and the radial direction were shown in Fig. 2a and 2b, respectively. The variation of the Zn concentration along the growth direction is very pronounced, 10% is the largest difference. However, the variation of the Zn concentration along the radial direction is less than 1%. In the case of the $Cd_{1-x-y}Zn_xMn_yTe$ quaternary compounds, shown in Fig. 3, the change of the molar fraction for the ingredient elements is similar to the results obtained for the ternary compounds. For both ternary and quaternary compounds, the maximum Zn concentration along the growth direction occurs at the place around 12 mm from the tip of the ingot.

To study the possibility of the usage as an optoelectronic device, the resistivity and etch pit density (the etchant consisting of H_2O(20 ml):H_2O_2(20

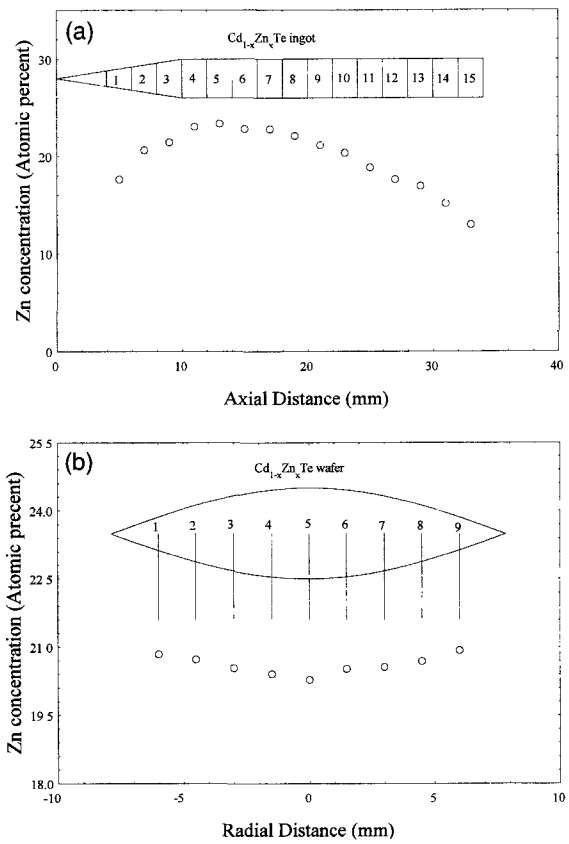

Fig. 2. (a) The Zn concentration versus the growth distance plot for the $Cd_{1-x}Zn_xTe$ crystal. (b) The Zn concentration versus the radial distance plot for the $Cd_{1-x}Zn_xTe$ crystal.

Table 1
The resistivity and etch pit density (EPD) for the $Cd_{1-x-y}Zn_xMn_yTe$ crystals

Sample		Resistivity ($\Omega \cdot$cm)	EPD (cm^{-2})
1:	$Cd_{0.96}Zn_{0.04}Te$	3.35×10^3	2.10×10^5
2:	$Cd_{0.88}Zn_{0.12}Te$	2.14×10^3	7.70×10^4
3:	$Cd_{0.86}Zn_{0.14}Te$	3.71×10^3	3.70×10^5
4:	$Cd_{0.80}Zn_{0.20}Te$	4.71×10^3	4.40×10^4
5:	$Cd_{0.983}Mn_{0.017}Te$	1.51×10^3	9.71×10^4
6:	$Cd_{0.927}Zn_{0.055}Mn_{0.018}Te$	3.13×10^3	3.00×10^4
7:	$Cd_{0.749}Zn_{0.225}Mn_{0.026}Te$	8.89×10^3	1.06×10^5
8:	$Cd_{0.524}Zn_{0.448}Mn_{0.028}Te$	7.34×10^4	5.18×10^4
9:	$Cd_{0.309}Zn_{0.667}Mn_{0.024}Te$	5.53×10^2	5.88×10^4
10:	$Cd_{0.094}Zn_{0.889}Mn_{0.016}Te$	4.28×10^2	1.05×10^4
11:	$Zn_{0.987}Mn_{0.013}Te$	1.59×10^2	1.24×10^4
12:	$Cd_{0.55}Zn_{0.40}Mn_{0.05}Te$ doped 1000 ppm Cl	3.71×10^7	–

ml) : HF(30 ml) was used) [13] of the $Cd_{1-x-y}Zn_xMn_yTe$ crystals were measured and are listed in Table 1. The $Cd_{1-x}Zn_xTe$ crystals are p-type with a resistivity of about 10^3 $\Omega \cdot$ cm and the EPD is around $10^4/cm^2$. With approximately 2% of Mn, both the resistivity and the EPD of the quaternary compound do not change significantly. The resistivity value obtained for the $Cd_{1-x-y}Zn_xMn_yTe$ is much higher than that obtained from the CdZnTe crystals grown by the sublimation and physical vapour transport method [14]. With the doping of chlorine, the resistivity of the quaternary compound can even be raised to 10^7 $\Omega \cdot$ cm.

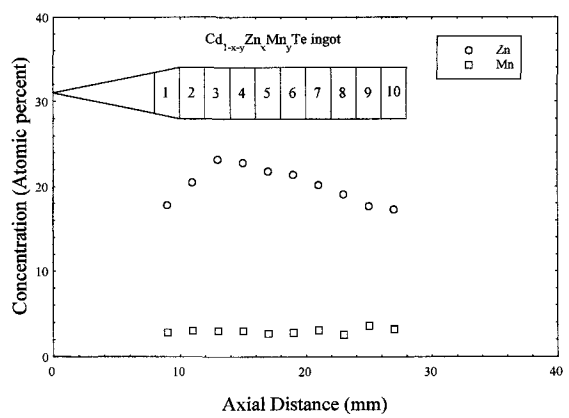

Fig. 3. The Zn (○) and Mn (□) concentration versus the growth distance plot for the $Cd_{1-x-y}Zn_xMn_yTe$ crystal.

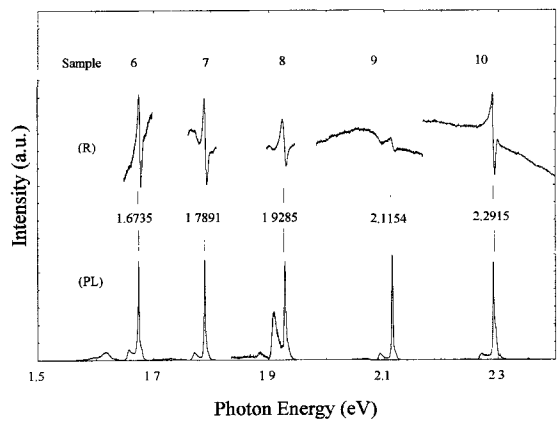

Fig. 4. The reflectivity and photoluminescence spectra for the $Cd_{1-x-y}Zn_xMn_yTe$ crystals.

In Fig. 4, the reflectivity (R) and photoluminescence (PL) spectra are shown. The near bandgap structures from the reflectivity spectra exhibit sharp excitonic transitions, which indicate very good optical quality for the $Cd_{1-x-y}Zn_xMn_yTe$ crystals. The nice optical quality of the grown crystals was further verified by the PL work. The full width at half maximum (FWHM) of the main peaks from the PL spectra for all the $Cd_{1-x-y}Zn_xMn_yTe$ crystals are about 4.2 meV, the same as that of the CdZnTe crystals.

In order to investigate the magnetic field sensitive optical properties, we have carried out the magneto-PL experiments. In Fig. 5, the magneto-PL spectra for the $Cd_{1-x-y}Zn_xMn_yTe$ crystals at 0, 2, 4, and 6 T are shown. The free exciton, marked as X, exhibits red shift in energy at non-zero magnetic field. The energy shift is as large as 12 meV/T at low magnetic field, and saturate at high magnetic field. Note that for the $Cd_{1-x-y}Zn_xMn_yTe$ crystals with 2% of Mn, the electrical properties do not noticeably change from their non-magnetic compounds. While, the magneto-optical properties of the two kinds of compound, non-magnetic $Cd_{1-x-y}Zn_xTe$ and magnetic $Cd_{1-x-y}Zn_xMn_yTe$, are extremely different. In Fig. 5, the impurity related structure, labelled as I, shows similar magnetic field dependent behaviour as the free exciton.

We have also measured the magnetization of the $Cd_{1-x-y}Zn_xMn_yTe$ crystals using a superconducting quantum interference device magnetometer. The

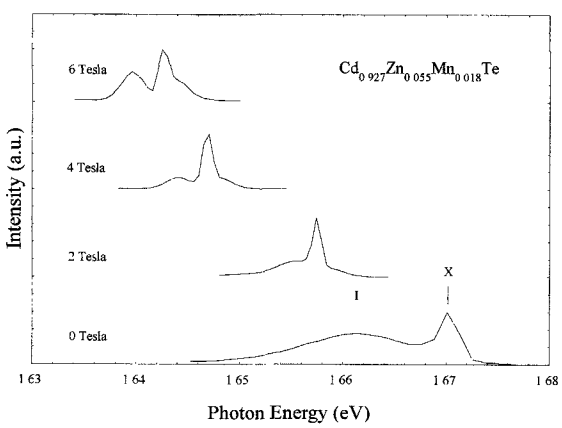

Fig. 5. The magneto-photoluminescence spectra from the $Cd_{0.927}Zn_{0.055}Mn_{0.018}Te$ crystal at 0, 2, 4 and 6 T.

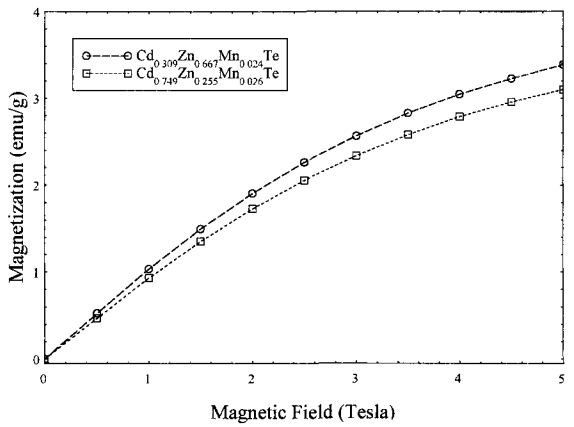

Fig. 6. The magnetization versus magnetic field plot for the $Cd_{0.309}Zn_{0.667}Mn_{0.024}Te$ (○) and $Cd_{0.749}Zn_{0.255}Mn_{0.026}Te$ (□) crystals.

representative magnetization versus magnetic field dependence is shown in Fig. 6 for the $Cd_{0.749}Zn_{0.225}Mn_{0.026}Te$ and $Cd_{0.309}Zn_{0.667}Mn_{0.025}Te$ crystals. The magnetization exhibits typical Brillouin magnetic behaviour. With the magnetization measurements and the magneto-optical studies, the exchange constant can be determined $N_0(\alpha - \beta) = 1.01$ eV for the $Cd_{0.309}Zn_{0.667}Mn_{0.025}Te$ crystal. This value is close to $N_0(\alpha - \beta) = 1.10$ eV [15] and 1.29 eV [16] for the CdMnTe and ZnMnTe crystals.

4. Conclusion

We have grown $Cd_{1-x-y}Zn_xMn_yTe$ crystals using the temperature gradient solution method. The sample quality of the $Cd_{1-x-y}Zn_xMn_yTe$ quaternary compounds are as good as the $Cd_{1-x}Zn_xTe$ ternary compound grown by the same method. The crystals are p-type and have a resistivity of $10^3\ \Omega \cdot cm$. The resistivity can be raised even to $10^7\ \Omega \cdot cm$ by doping with chlorine. It is natural to conclude that the quaternary compounds, which have the same quality as the ternary compounds, have potential applications in optoelectronic devices. Furthermore, the typical magnetic and magneto-optical properties of the quaternary compounds render the $Cd_{1-x-y}Zn_xMn_yTe$ crystals as possible candidates for the magnetic field sensitive sensor.

Acknowledgements

This work was supported by the National Science Council, Taiwan, ROC, by the contract numbers NSC-84-2112-M-033-005 and NSC-84-0208-M-033-001.

References

[1] J.K. Furdyna, J. Appl. Phys. 64 (1988) R29.
[2] J.K. Furdyna and J. Kossut, Eds., Semiconductors and Semimetals, Vol. 25 (Academic Press, New York, 1988).
[3] L.P. Fu, T. Schmiedel, A. Petrou, J. Warnock and B.T. Jonker, Appl. Phys. Lett. 60 (1992) 583.
[4] W.C. Chou, A. Petrou, J. Warnock and B.T. Jonker, Phys. Rev. Lett. 67 (1991) 3820.
[5] D.D. Awschalom, M.R. freeman, N. Samarth, H. Luo and J.K. Furdyna, Phys. Rev. Lett. 66 (1991) 1212.
[6] S. von Molnar, A. Briggs, J. Flouguet and G. Remenyi, Phys. Rev. Lett. 51 (1983) 706.
[7] A. Twardowski, C.J.M. Denissen, W.J.M. de Jonge, A.T.A.M. de Waele, M. Demianiuk and R. Triboulet, Solid State Commun. 59 (1986) 199.
[8] A. Twardowski, Y.F. Chen, W.C. Chou and M. Demianiuk, Solid State Commun. 90 (1994) 493.
[9] Y. Irie, T. Sato and E. Ohta, Phys. Rev. B 51 (1995) 13084.
[10] E. Oh, R.G. Alonso, I. Miotkowski and A.K. Ramdas, Phys. Rev. B 45 (1992) 10934.
[11] H. Gurrero, J.L. Escudero and E. Bernabeu, Sensors Actuators A 39 (1993) 25.
[12] L.R. Shiozawa and J.M. Jost, Research on Improved II–VI Crystals, Aerospace Research Laboratories, ARL 71-0017 (1971) pp. 19, 21.
[13] K. Nakagawa, K. Maeda and S. Takeuchi, Appl. Phys. Lett. 34 (1979) 574.
[14] J.L. Boone, G. Cantwell, W.C. Harsch, J.E. Thomas and B.A. Foreman, J. Crystal Growth 139 (1994) 27.
[15] J.A. Gaj, R. Planel and G. Fishman, Solid State Commun. 29 (1979) 435.
[16] A. Twardowski, M. von Ortenberg, M. Demianiuk and R. Pauthenet, Solid State Commun. 51 (1984) 849.